Manganese Oxidation by Modified Reaction Centers from *Rhodobacter sphaeroides*†

L. Kálmán,‡,§ R. LoBrutto,# J. P. Allen,*,‡ and J. C. Williams‡

Department of Chemistry and Biochemistry and Department of Plant Biology, Arizona State University, Tempe, Arizona 85287-1604

Received May 8, 2003; Revised Manuscript Received July 22, 2003

ABSTRACT: The transfer of an electron from exogenous manganese (II) ions to the bacteriochlorophyll dimer, P, of bacterial reaction centers was characterized for a series of mutants that have P/P^+ midpoint potentials ranging from 585 to 765 mV compared to 505 mV for wild type. Light-induced changes in optical and EPR spectra of the mutants were measured to monitor the disappearance of the oxidized dimer upon electron donation by manganese in the presence of bicarbonate. The extent of electron transfer was strongly dependent upon the P/P^+ midpoint potential. The midpoint potential of the Mn^{2+}/Mn^{3+} couple was calculated to decrease linearly from 751 to 623 mV as the pH was raised from 8 to 10, indicating the involvement of a proton. The electron donation had a second order rate constant of approximately 9×10^4 M^{-1} s^{-1}, determined from the linear increase in rate for Mn^{2+} concentrations up to 200 μM. Weak dissociation constants of 100−200 μM were found. Quantitative EPR analysis of the six-line free Mn^{2+} signal revealed that up to seven manganese ions were associated with the reaction centers at a 1 mM concentration of manganese. The association and the electron transfer between manganese and the reaction centers could be inhibited by Ca^{2+} and Na^+ ions. The ability of reaction centers with high potentials to oxidize manganese suggests that manganese oxidation could have preceded water oxidation in the evolutionary development of photosystem II.

Energy conversion in photosynthesis takes place in membrane-bound pigment-protein complexes known as reaction centers in bacteria and photosystems I and II in plants, algae, and cyanobacteria. In these complexes, the (bacterio)-chlorophyll molecules that form the primary electron donor absorb light energy and are rapidly oxidized to a cation radical following electron transfer to a series of acceptors. The generated electrical potentials are converted into transmembrane ion potentials by migration of the oxidizing and reducing equivalents to the cytochrome b_6f and bc_1 complexes, resulting in an electrochemical potential that is utilized for ATP synthesis.

The bacterial reaction center and photosystem II show structural homology, but the two systems function differently at the electron donor side of the membrane. In reaction centers from *Rhodobacter sphaeroides*, the secondary donor to the oxidized primary donor P^+ is a water-soluble cytochrome c_2 molecule (*1*). In photosystem II, the secondary donor is a redox active tyrosine, Y_Z, that in turn oxidizes the manganese cluster, with oxygen liberated after four oxidation equivalents are transferred (reviewed in ref *2*). Wild-type reaction centers are not able to oxidize tyrosine or manganese. The wild-type P/P^+ midpoint potential[1] is ∼0.5 V (*3*−*5*), at least 0.25 V lower than the observed oxidation−reduction potentials of tyrosines in solution or in other proteins (for review see ref *6*) and 0.13−0.42 V lower than the midpoint potential of the Mn^{2+}/Mn^{3+} couple in different bicarbonate complexes (*7*). The high midpoint potential of ∼1 V for the primary donor in photosystem II is a key functional attribute in the oxidation of water.

By changing the hydrogen-bonding pattern of the bacteriochlorophyll dimer in reaction centers, the P/P^+ midpoint potential can be altered (*5*). Single mutations that introduce an additional hydrogen bond to P increase the midpoint potential by 0.06−0.125 V. For example, the mutant with the change Leu to His at L131, called the LH(L131) mutant, has a P/P^+ midpoint potential 0.085 V higher than wild type. Mutants with several changes show additive increases in the midpoint potential. The introduction of three hydrogen bonds in the triple mutant, LH(L131)+LH(M160)+FH(M197), results in a midpoint potential of 0.76 V. In this work, we investigate whether Mn^{2+} can serve as a secondary electron donor to P^+ in mutants with altered midpoint potentials. Since bicarbonate has been proposed to play a role in the photoactivation of the manganese cluster of photosystem II (*8*−*11*), the influence of bicarbonate on this reaction was tested.

† This work was supported by Grant MCB 0131764 from the NSF, and L.K. was partially supported by the Astrobiology Institute.

* Corresponding author. Phone: 480−965−8241. Fax: 480−965−2747. E-mail: jallen@asu.edu.

‡ Department of Chemistry and Biochemistry.

Department of Plant Biology.

§ Permanent address: Department of Biophysics, University of Szeged, Egyetem u.2, H-6722, Szeged, Hungary.

[1] Abbreviations: P, bacteriochlorophyll dimer; Q_A and Q_B, primary and secondary quinones, respectively; Hepes, *N*-[2-hydroxyethyl]-piperazine-*N*′[2-ethane]sulfonic acid; Ches, (2-[*N*-cyclohexylamino]-ethane sulfonic acid.

10.1021/bi034747o CCC: $25.00
Published on Web 08/29/2003

MATERIALS AND METHODS

Protein Isolation. The mutants containing alterations in the genes encoding the L and M subunits of reaction centers from *Rb. sphaeroides* have been previously described (*5*). Cells were grown semiaerobically, and the reaction centers were prepared as described earlier (*12*), except that Triton X-100 was used for the ion exchange chromatography step instead of LDAO, and EDTA was removed by a long (24 h) dialysis.

Optical Spectroscopy. A Cary 5 spectrophotometer (Varian) was utilized to measure the light-induced optical difference spectra. Illumination of the samples was achieved by using an Oriel tungsten lamp with an 860 ± 15 nm interference filter. The spectral changes were measured in the near-infrared region between 700 and 1000 nm. A single beam spectrometer of local design (*13*) was used to measure the kinetics of the primary donor recovery. The reaction centers were excited at 532 nm with a 5 ns laser pulse width using a ND:YAG laser (Continuum). The observation wavelength was set to the maximum of the Q_y transition of the dimer band, at approximately 865 nm depending on the mutant. A nonlinear least-squares method was used to fit the data. For the steady-state optical measurements, the reaction centers were at a concentration of 1.5 μM in 15 mM buffer (Hepes, Tris, or Ches depending on pH), 15 mM $NaHCO_3$, 0.05% Triton X-100, 20 mM NaCl, and 100 μM terbutryne. In the flash-induced optical measurements, 10-fold excess ubiquinone was added, and terbutryne was absent, for better decomposition of the kinetic phases. The optical measurements were carried out at room temperature.

EPR Spectroscopy. The EPR measurements were performed using a Bruker E580 X-band spectrometer with a magnetic field modulation frequency of 100 kHz, an amplitude of 0.4 mT, a microwave power of 10 mW, and a microwave frequency of approximately 9.64 GHz. Samples were placed in a quartz flat cell, which was mounted in a Bruker TE_{102} rectangular standard cavity, at ambient temperature. The spectra were obtained by averaging several scans. Reaction centers were concentrated for the EPR measurements in a Centricon micro-concentrator (Amicon) up to 300 μM. No bicarbonate was used for the EPR measurements carried out without illumination because the complexation of Mn^{2+} with bicarbonate reduces the intensity of the six-line free Mn^{2+} signal.

RESULTS

Spectral Changes due to Manganese. In the absence of manganese, the light-minus-dark optical spectra of the mutants were similar to wild type. For example, the light-induced changes in the optical spectrum of the triple mutant LH(L131)+LH(M160)+FH(M197) exhibited characteristic features associated with both the oxidized dimer and the reduced primary quinone (Figure 1A). These changes include an absorption decrease in the dimer band centered at 865 nm, an electrochromic blue shift on the bacteriochlorophyll monomer region around 800 nm due to the positive charge on the oxidized dimer, and an electrochromic red shift on the bacteriopheophytin band around 760 nm as a result of the negative charge on the reduced quinone.

Addition of 1 mM $MnCl_2$ in the presence of excess bicarbonate (HCO_3^-) changed the light-induced optical spectrum of the triple mutant dramatically (Figure 1A). The features associated with the oxidized dimer are no longer present, and only signals characteristic of the reduced primary quinone are evident, indicating that Mn^{2+} serves as a secondary electron donor to P^+. The reaction was accompanied by formation of a brown precipitate, most probably due to formation of Mn (IV)-oxide or Mn (IV)-carbonate as a result of disproportionation of the product Mn^{3+} to Mn^{2+} and Mn^{4+}. Addition of manganese had no effect on the light-induced spectrum of wild-type reaction centers (data not shown). The effect of Mn^{2+} could be suppressed by addition of Ca^{2+} or Na^+ in excess concentration (data not shown for Na^+).

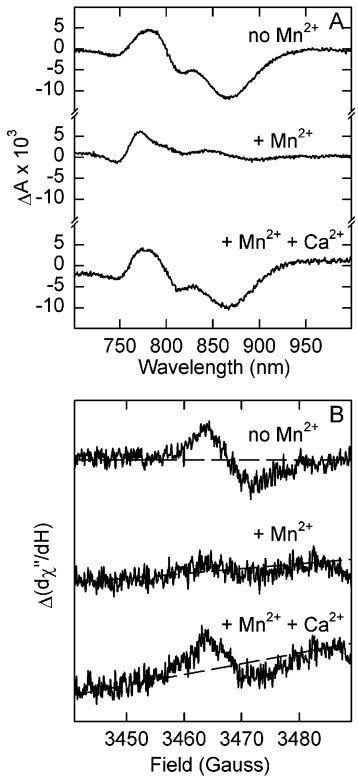

FIGURE 1: Effect of Mn^{2+} and Ca^{2+} on the near-infrared light-minus-dark difference absorption spectra (A) and EPR spectra (B) of the LH(L131)+FH(M197)+LH(M160) triple mutant at pH 9.0. Upper traces in both panels are the spectra without $MnCl_2$, middle traces are those with excess $MnCl_2$ and the lower traces are those with $MnCl_2$ and $CaCl_2$. The lack of the characteristic optical and EPR features of the oxidized dimer in the presence of Mn^{2+} (middle traces) likely results from the reduction of P^+ by manganese. Addition of Ca^{2+} in excess concentration suppresses the effect of Mn^{2+} (bottom traces), restoring the features observed in spectra without Mn^{2+}. Conditions: 1.5 μM reaction centers for the optical measurements and 50 μM reaction centers for the EPR measurements suspended in 0.05% Triton X-100, 15 mM Ches, pH 9.0, 15 mM $NaHCO_3$, 100 μM terbutryne. Middle traces: +1 mM $MnCl_2$; bottom traces: +1 mM $MnCl_2$ +20 mM $CaCl_2$. Illumination conditions were as described in Materials and Methods. The drift in the baseline of the light-minus-dark EPR spectra in the presence of manganese is due to the large background signal of Mn^{2+} (see Figure 5).

The presence of P^+ was monitored by measurement of light-induced EPR spectra of the triple mutant in the absence and presence of externally added Mn^{2+} ions (Figure 1B). Without manganese, the characteristic spectrum of the cation radical of the bacteriochlorophyll dimer was detected in the $g = 2.0$ region. In the presence of excess Mn^{2+}, the P^+ signal diminished. Addition of Ca^{2+} canceled the effect of Mn^{2+}.

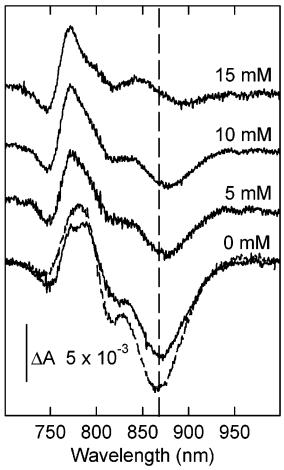

FIGURE 2: Dependence of the P^+ reduction by Mn^{2+} on bicarbonate concentration. The light-minus-dark optical difference spectra of reaction centers from the LH(L131)+FH(M197)+LH(M160) triple mutant at different bicarbonate concentrations in the presence of 1 mM $MnCl_2$ (solid lines) are compared to the spectrum of reaction centers without both Mn^{2+} and bicarbonate (dashed line). The extent of the oxidized dimer, monitored as the absorption change at 865 nm, decreases with increasing bicarbonate concentration. The dimer band position is indicated with a vertical dashed line for guidance. Conditions as in Figure 1.

Similarly, the amplitude of the Mn^{2+} signal decreased after illumination when reaction centers were present (data not shown). The changes in the EPR spectra are consistent with electron transfer from manganese to the oxidized dimer, in accordance with the optical measurements.

The extent of the alteration due to manganese in the light-minus-dark optical spectrum was dependent on the concentration of bicarbonate. In the absence of externally added bicarbonate only partial (40%) reduction of P^+ was observed when manganese was added (Figure 2). As the bicarbonate concentration was increased, the amount of P^+ decreased, with the maximum effect achieved at 15 mM bicarbonate. In the absence of manganese, bicarbonate had no effect on the spectrum.

Rate of Manganese Oxidation by P$^+$. The recovery of the oxidized dimer after a saturating laser flash was measured at 865 nm in Q_B reconstituted samples at pH 9.4. In the absence of Mn^{2+}, a major component with a rate of 5 s^{-1} and a minor component (6%) with a rate of 15 s^{-1} were measured for the LH(L131)+FH(M197) double mutant (Figure 3A). Under these conditions, P^+ decays predominantly through charge recombination from $P^+Q_B^-$, so the major component was assigned to this electron-transfer reaction. The minor component was attributed to charge recombination from $P^+Q_A^-$ in reaction centers that lack Q_B due to incomplete reconstitution. These designations were confirmed by the observation that in the presence of terbutryne, which displaces Q_B, the component with the rate of 15 s^{-1} predominated, and the component with the rate of 5 s^{-1} was not observed. The charge recombination rates are faster than those found in wild-type reaction centers because both the $P^+Q_B^-$ and the $P^+Q_A^-$ charge recombination rates are dependent upon the P/P^+ midpoint potential (*14*).

The addition of Mn^{2+} had a clear effect on the decay rate (Figure 3A). In the presence of Mn^{2+}, the kinetic traces were decomposed into three exponential components (Figure 3B). Two of these components had rates corresponding to the

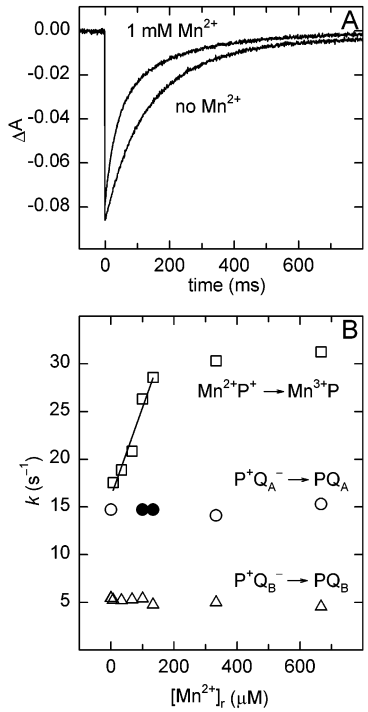

FIGURE 3: Kinetics of Mn^{2+} oxidation in reaction centers from the LH(L131)+FH(M197) double mutant. (A) Representative kinetic traces of the P^+ recovery after flash excitation monitored at 865 nm with and without added Mn^{2+}. (B) In the presence of Mn^{2+}, P^+ reduction can be resolved into three components. The fastest component is assigned to P^+ reduction by Mn^{2+} (squares). For concentrations less than 200 μM, the rate of this component was linearly dependent upon the Mn concentration, yielding a second-order rate constant of 9.58×10^4 M^{-1} s^{-1}. The rates of the other two components were independent of the Mn^{2+} concentration and are attributable to charge recombination from $P^+Q_A^-$ (circles) and $P^+Q_B^-$ (triangles). At Mn^{2+} concentrations of 100 and 133 μM, the $P^+Q_A^-$ charge recombination contribution (closed circles) could not be resolved, so the fit was required to have a component with a rate of 14.7 s^{-1}, and at lower Mn^{2+} concentrations this component could not be resolved. The Mn^{2+} concentration shown, $[Mn^{2+}]_r$, is the relative concentration for 1 μM reaction centers. Conditions as in Figure 1, except pH 9.4 and no terbutryne added.

$P^+Q_A^-$ and $P^+Q_B^-$ charge recombination rates. These rates were independent of Mn^{2+} concentration, and the relative amplitudes of these components decreased as the Mn^{2+} concentration increased. The fastest component had a rate that increased from approximately 17 to 30 s^{-1} as the Mn^{2+} concentration increased to 200 μM (Figure 3B). Above 200 μM, the rate for this component was independent of the Mn^{2+} concentration. The relative amplitude of the fastest component was correlated with the Mn^{2+} concentration (Figure 4A). This component was assigned as arising from reduction of P^+ by Mn^{2+}.

A bimolecular rate constant for Mn^{2+} oxidation was determined in the region where the rate increased linearly with Mn^{2+} concentration (Figure 3B). The fit of the regression lines yielded values of 9.58×10^4 and 9.16×10^4 M^{-1} s^{-1} for the LH(L131)+FH(M197) and (LH(M160)+FH(M197) double mutants, respectively. The effect of Mn^{2+} was less evident in the other mutants due to either a smaller amount of P^+ reduction or a smaller difference between the charge recombination rate from the quinones and the rate associated with oxidation of Mn^{2+}.

Dependence of P$^+$ Reduction on Manganese Concentration. The changes in the steady-state, light-minus-dark optical

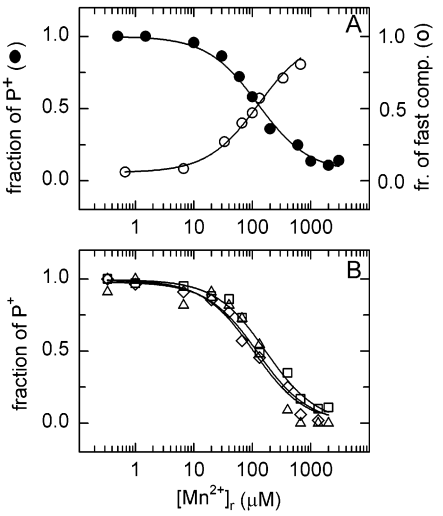

FIGURE 4: Dependence of the fraction of P^+ in reaction centers from mutants with highly oxidizing bacteriochlorophyll dimers on added Mn^{2+} concentration. The P^+ content was determined from light-minus-dark difference spectra for the LH(L131)+FH(M197) double mutant (A) and the LH(L131)+FH(M197)+LH(M160) triple mutant (B). The fraction of the fast component in the recovery kinetics of the flash-induced oxidized dimer (A, right axis) increases in the same manner as P^+ decreases upon changing the Mn^{2+} concentration at pH 9.4. For the triple mutant, the measurements were made at pH 8.0 (squares), pH 9.0 (triangles), and pH 9.4 (diamonds). The data were fit with the binding equation: fraction of $P^+ = 1 - \{A/(1 + K_D/[Mn^{2+}]_r)\}$, where A is the amplitude of the change, K_D is the dissociation constant and $[Mn^{2+}]_r$ is the relative concentration of added $MnCl_2$ for 1 μM reaction centers. The resulting K_D values are 126 and 122 μM determined from the steady-state and kinetic measurements, respectively, for the double mutant at pH 9.4, and 170, 124, and 106 μM at pH 8.0, 9.0, and 9.4, respectively, for the triple mutant. The average error of the fit is $\pm$ 20 μM. Conditions: as in Figure 1 except the pH was varied and the reaction center concentrations were 1 or 1.5 μM.

spectra due to manganese were measured for two mutants for a range of Mn^{2+} concentrations. The fraction of P^+, as determined by the extent of absorption at 865 nm, was found to decrease as the manganese concentration increased for the LH(L131)+FH(M197) double mutant at pH 9.4 (Figure 4A). This dependence of the fraction of P^+ on the manganese concentration could be fit assuming that the manganese bound only weakly, with an apparent dissociation constant of approximately 126 μM. In the kinetic measurements described above, the fraction of the fast component was found to increase with increasing manganese concentration. This dependence could also be fitted with an apparent dissociation constant of approximately 122 μM. Thus, two independent measurements were found to yield essentially the same dissociation constant.

The fraction of P^+ in the presence of different manganese concentrations was also determined from light-minus-dark optical spectra for the LH(L131)+FH(M197)+LH(M160) triple mutant at different pH values (Figure 4B). At pH 9.4, the dependence could be fitted with an apparent dissociation constant of 106 μM, comparable to the apparent dissociation constant determined for the double mutant. The dependence of the fraction of P^+ on the manganese concentration was similar at pH 8.0, 9.0, and 9.4.

Determination of Mn^{2+} Binding by EPR Spectroscopy. The association of Mn^{2+} with reaction centers was assessed by changes in the amplitude of the Mn^{2+} EPR signal in the

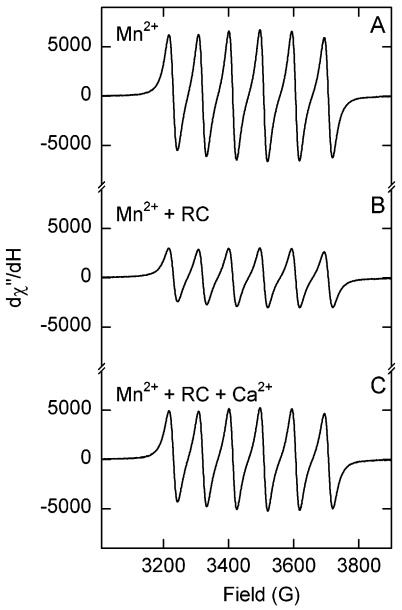

FIGURE 5: Room-temperature X-band EPR spectra of $MnCl_2$. (A) A solution of 1 mM $MnCl_2$ in 0.05% Triton X-100, 15 mM Ches, pH 9.0, and 20 mM NaCl displays a six-line Mn^{2+} signal. (B) The addition of 73 μM reaction centers from the triple mutant significantly reduced the amplitude of the Mn^{2+} EPR signal. (C) Addition of both 73 μM reaction centers and 30 mM $CaCl_2$ resulted in an EPR signal with an amplitude comparable to that of 1 mM $MnCl_2$ alone.

presence of reaction centers (*15*). The peak-to-peak amplitude of the characteristic six-line Mn^{2+} spectrum in the $g = 2.00$ region was measured to determine the amount of free manganese (Figure 5). The amplitude of the Mn^{2+} signal diminished 2-fold after the addition of reaction centers. The 2-fold reduction in Mn^{2+} concentration corresponds to a loss of 500 μM Mn^{2+} from solution, presumably due to binding to the protein. Since the reaction centers are at a concentration of 73 μM, at most seven Mn^{2+} are associated with each reaction center. This calculation represents a maximal limit due to uncertainties in estimating the amount of Mn^{2+} associated with the detergent micelles and a limited stability of Mn^{2+} in the detergent solution. The bound Mn^{2+} could be released from the reaction centers by the addition of 20 mM $CaCl_2$. Similar effects were seen with the use of NaCl. The effect of Ca^{2+} or Na^+ may be to generally alter the electrostatic nature of the surface rather than competing with Mn^{2+} at specific sites.

Oxidation/Reduction Midpoint Potential of the Mn^{2+}/Mn^{3+} Couple. The reduction of P^+ by manganese was measured in reaction centers with midpoint potentials ranging between 505 and 765 mV. The extent of the light-induced optical difference spectrum at 865 nm was measured upon addition of 1 mM $MnCl_2$ at pH values ranging from 7.0 to 10.4. Under these conditions, the use of 1 mM $MnCl_2$ represents an excess concentration based upon the apparent dissociation constants described above. The oxidation of Mn^{2+} by P^+ was found to be strongly dependent on the P/P^+ midpoint potential (Figure 6A). At each pH, the fraction of P^+ remaining was found to decrease as the P/P^+ midpoint potential of the mutants increased. For each mutant, the fraction of P^+ remaining decreased as the pH increased from 8 to 10. The pH range could not be extended, as above pH 10 the reversibility and the reproducibility of the measurements

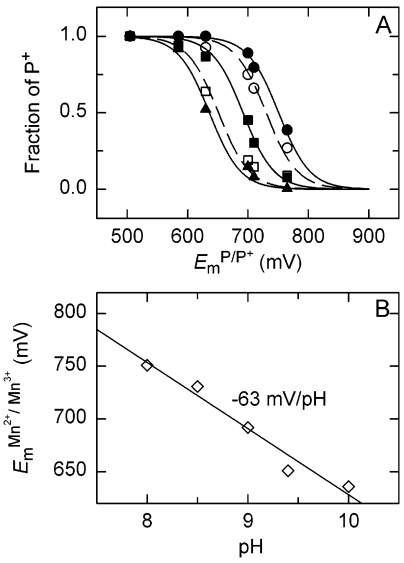

FIGURE 6: Determination of the Mn^{2+}/Mn^{3+} redox midpoint potential. (A) The fraction of P^+ in light-minus-dark spectra in the presence of excess Mn^{2+} at pH 8.0 (closed circles), pH 8.5 (open circles), pH 9.0 (closed squares), pH 9.4 (open squares), and pH 10.0 (closed triangles) was determined for reaction centers from wild type and the mutants LH(L131), FH(M197), LH(M160)+FH(M197), LH(L131)+FH(M197), and LH(L131)+FH(M197)+LH(M160), having P/P^+ midpoint potentials (E_m^{P/P^+}) of 505, 585, 630, 700, 710, and 765 mV, respectively (*5*). At each pH, the value of $E_m^{Mn^{2+}/Mn^{3+}}$ was determined from a fit using eq 3. (B) The values of $E_m^{Mn^{2+}/Mn^{3+}}$ were found to have a linear dependence on pH, with a slope of −63 mV/pH. Conditions: 1.5 μM reaction centers, 0.05% Triton X-100, 15 mM buffer (Tris or Ches depending on pH), 15 mM $NaHCO_3$, 100 μM terbutryne. $MnCl_2$ was used at a concentration of 1 mM.

became poor, mainly due to the instability of the manganese compounds, while below pH 8 no spectral features associated with oxidation of manganese were observed.

The increase in the observed manganese oxidation as the P/P^+ midpoint potential (E_m^{P/P^+}) increases likely arises from the resultant increase in the free energy difference ($\Delta G°$) for the oxidation reaction. The free energy difference is related to the difference between E_m^{P/P^+} and $E_m^{Mn^{2+}/Mn^{3+}}$, the Mn^{2+}/Mn^{3+} midpoint potential, by

$$\Delta G° = -nF(E_m^{P/P^+} - E_m^{Mn^{2+}/Mn^{3+}}) \quad (1)$$

where n is the number of electrons, in this case 1, and F is the Faraday constant. The free energy difference, assuming the equilibrium $[P^+Mn^{2+}] \leftrightarrow [PMn^{3+}]$, also determines the equilibrium constant, or equivalently the ratio $[PMn^{3+}]/[P^+Mn^{2+}]$. This ratio can be obtained from the experimental measurement of the fraction of P^+ remaining, assuming that $[P^+] + [P] = 1$. The dependence of $\Delta G°$ on the fraction of P^+ remaining is given by

$$\Delta G° = -RT \ln \frac{[P]}{[P^+]} \quad (2)$$

where R is the gas constant and T is the temperature. Combining eqs 1 and 2 yields the following relationship:

$$E_m^{Mn^{2+}/Mn^{3+}} = E_m^{P/P^+} - \frac{RT}{nF} \ln \frac{[P]}{[P^+]} \quad (3)$$

This equation has the form of the Nernst equation and provides a means of relating the fraction of P^+ remaining to the P/P^+ and Mn^{2+}/Mn^{3+} midpoint potentials.

At each pH, the data were fit with eq 3 to yield $E_m^{Mn^{2+}/Mn^{3+}}$. The value of $E_m^{Mn^{2+}/Mn^{3+}}$ decreased with increasing pH, from 751 mV at pH 8.0 to 636 mV at pH 10.0 (Figure 6B). The calculated values of $E_m^{Mn^{2+}/Mn^{3+}}$ show a dependence of −63 mV/pH. This calculation does not include a small correction due to the weak pH dependence of E_m^{P/P^+} observed in wild-type reaction centers (*16*, *17*). Assuming that the mutants have the same dependence of E_m^{P/P^+} on pH as wild type, correcting the values of E_m^{P/P^+} for this dependence results in a slight increase in the dependence of the calculated $E_m^{Mn^{2+}/Mn^{3+}}$ on pH to −69 mV/pH. In either case, the pH dependence of $E_m^{Mn^{2+}/Mn^{3+}}$ is comparable to a dependence of −60 mV/pH, which would indicate the participation of one proton in the redox reaction.

DISCUSSION

Elevating the P/P^+ midpoint potential in bacterial reaction centers should render them capable of reactions that are not possible in wild type. For example, reaction centers with highly oxidizing bacteriochlorophyll dimers have been shown previously to be able to oxidize tyrosine (*18*, *19*). In this work, reaction centers with elevated midpoint potentials exhibited spectral changes that indicate that these reaction centers are capable of oxidizing manganese. The electron donation reaction was highly dependent upon the midpoint potential of the dimer, the pH, and the concentrations of Mn^{2+} and bicarbonate. The effects of these parameters on the electron transfer are discussed below, as well as the implication of the results for other relevant biological systems, especially the evolutionarily related photosystem II.

Spectral Changes in the Presence of Manganese. The presence of manganese had no effect on the optical light-minus-dark difference spectrum of wild type. In striking contrast, mutants with increased midpoint potentials show the loss of the absorption changes associated with the oxidized electron donor when manganese is present. For example, upon illumination of the triple mutant without the presence of Mn^{2+} (Figure 1) the optical spectra show the characteristic changes associated with both the oxidized dimer and the reduced quinone (*20*). In the presence of excess Mn^{2+}, the spectra lack the features of the oxidized dimer and are identical with the spectra assigned to the Q_A^-/Q_A transition (*21*). The optical changes in the presence of Mn^{2+} are characteristic of the presence of a secondary electron donor to P^+. Similarly, in the presence of manganese, the P^+ signal is absent from the EPR spectra. Together these results demonstrate that P^+ is reduced in the presence of Mn^{2+} in these reaction centers.

Midpoint Potential Dependence. Measurements of mutants with different P/P^+ midpoint potentials show that the electron transfer from manganese to the oxidized dimer is a well-defined reaction that is dependent upon the driving force. At any given pH, the free energy difference for electron transfer is given by the difference in the midpoint potentials of the manganese and P (eq 1). Thus, the largest extent of P^+ reduction by manganese is observed for the triple mutant,

which has the highest P/P^+ midpoint potential and correspondingly the largest free energy difference. In contrast, the wild type, with the lowest P/P^+ midpoint potential, shows no reduction, as expected from the unfavorable energetics of the reaction. For each mutant, the extent of P^+ reduction increased as the pH increased, and an approximately 60 mV/pH dependence of the manganese midpoint potential was determined. This pH dependence suggests the involvement of a proton in the electron-transfer reaction, which, since the protonational changes associated with the reduction of P^+ are small (*16*), probably results from the loss of a proton from the manganese−bicarbonate compound to the bulk solution upon oxidation of Mn^{2+} to Mn^{3+}.

Association between Manganese and the Reaction Center. The results indicate that manganese becomes associated with the reaction center at high concentrations but is not tightly bound. The linear dependence of the rate of P^+ reduction on the manganese concentration at concentrations less than 200 μM suggests a second-order mechanism in which the reaction rate is determined by the diffusion of Mn^{2+} to P^+ (Figure 3B). At higher concentrations, the independence of the rate on manganese concentration indicates an association of the manganese with the reaction center. The relatively high dissociation constants of 100 and 200 μM determined from several measurements (Figure 4) are consistent with the manganese not being tightly coordinated to the reaction center. It is likely that manganese ions can interact electrostatically at several locations on the reaction center surface most probably involving carboxylic residues. In addition to providing a Mn^{2+} ion close to P^+, the association of the manganese with the reaction center is expected to alter the Mn^{2+}/Mn^{3+} midpoint potential, making oxidation more favorable. The EPR measurements showing a loss of free manganese when reaction centers are present indicate that there are several such sites on the reaction center (Figure 5). One of these sites may be near the secondary quinone as indicated by changes in electron-transfer rates involving the quinones in the presence of Mn^{2+} in high concentration (*22*). The periplasmic surface near the dimer could also have such sites; however, achieving a tight binding site will require additional modification of the bacterial reaction center.

Comparison of the Rate of Manganese Oxidation with Other Systems. In photosystem II, the bound Mn cluster is oxidized by the intermediate electron carrier, $Y_Z^\bullet$ with a rate of up to 2×10^4 s^{-1} (*23*). Preparations of photosystem II in which the manganese cluster has been removed have also been used to characterize the kinetics of manganese oxidation (*24*, *25*). In these preparations, manganese oxidation occurs with a second-order rate of $\sim 6 \times 10^6$ M^{-1} s^{-1} (*15*). The second-order rate of $\sim 9 \times 10^4$ M^{-1} s^{-1} measured for the high potential reaction centers (Figure 3B) is much slower. The faster rate in photosystem II probably reflects a diffusion that is enhanced by electrostatic interactions at the manganese binding site. The significantly larger driving force for photosystem II compared to 0.05−0.12 eV for the reaction center mutants probably also contributes to the difference in rate. In Ru−Tyr−$(Mn)_2$ model systems, which resemble the $P_{680}-Y_Z-(Mn)_4$ triad, manganese oxidation by the tyrosyl radical is on the tens of milliseconds time scale, although the driving force is not the rate-limiting step (reviewed in ref *26*).

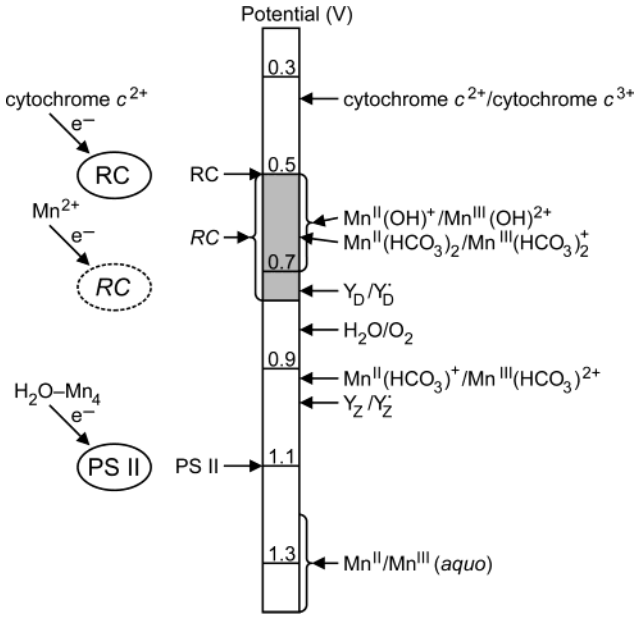

FIGURE 7: Comparison of the midpoint potentials of primary and secondary electron donors in bacterial reaction centers (RC) and photosystem II (PSII). Genetically modified bacterial reaction centers (denoted as *RC*) with elevated P/P^+ midpoint potentials (shaded potential range) can utilize manganese compounds as secondary electron donors. Reaction centers that utilize manganese as a secondary electron donor may have been an evolutionary precursor to photosystem II.

Role of Bicarbonate. The Mn^{2+}/Mn^{3+} midpoint potential is approximately 1.2 V for the hexa-aquo complex, clearly too high to be oxidized by the high potential reaction center mutants, while manganese−bicarbonate complexes have potentials that are significantly lower than the aquo form (*9*, *27*). Thus, the greater extent of P^+ reduction by Mn^{2+} in the presence of excess bicarbonate (Figure 2) may be due to the electrochemical stabilization of Mn^{3+} upon coordination with bicarbonate. The partial reduction of P^+ by Mn^{2+} without added bicarbonate may be to some extent due to the availability of ambient bicarbonate dissolved in the buffers at concentrations that can be estimated to be 4−50 μM under these conditions (*27*, *28*). In photosystem II, bicarbonate has an effect on electron-transfer involving two different sites. At the acceptor site, bicarbonate facilitates the transfer of an electron between the primary and the secondary plastoquinone (*29*). At the donor site of photosystem II, bicarbonate enhances the photoinduced assembly of the manganese cluster, suggesting that bicarbonate binds directly to the manganese ions (*10*, *11*).

Evolutionary Implications. Manganese could serve as an electron donor in photosynthetic organisms (Figure 7), and this may have been an intermediate step in the evolution of water oxidation at a manganese complex (*8*, *30*−*32*). Manganese is often found in surface layers of sediments, and its widescale availability would have provided primitive photosynthetic organisms with an electron source and a special ecological niche. Many different microorganisms, including bacteria, cyanobacteria, algae, yeast, and fungi can either oxidize or reduce manganese, and such activity plays a major role throughout natural environments ranging from fresh and marine waters to deep sea vents and desert climates (*33*). Manganese oxidation pathways in biological systems are diverse, and some are indirect; for example, manganese

oxidation occurs due to the production of hydrogen peroxide in some bacteria. To date, the capability of manganese oxidation has not been demonstrated in anoxygenic photosynthetic bacteria; however, support for the concept of direct metal oxidation is provided by the ability of a number of bacteria to oxidize iron under photosynthetic conditions (*34*).

The achievement of a highly oxidizing donor provides the reaction centers with a sufficient oxidation potential for water oxidation, but the conversion of H_2O to O_2 requires the ability to collect four electron equivalents. In the water-oxidizing complex, these equivalents are collected at the manganese cluster. To mimic this functional ability of the water−oxidation complex, it would be necessary to bind a metal cluster near the dimer such that it can serve as a secondary donor. Because many properties of the manganese cluster in photosystem II remain elusive, the development of a metal cluster that can perform this new electron-transfer process is a challenge.

ACKNOWLEDGMENT

We thank Drs. Charles Yocum and Tyler Caudle for stimulating discussions.

REFERENCES

1. Prince, R. C., Cogdell, R. J., and Crofts, A. R. (1974) *Biochim. Biophys. Acta 347*, 1−13.
2. Britt, R. D. (1996) in *Oxygenic Photosynthesis: The Light Reactions* (Ort, D. R., Yocum, C. F., Eds.) pp 137−164, Kluwer Academic Publishers, Dodrecht, The Netherlands.
3. Dutton, P. L., and Jackson, J. B. (1972) *Eur. J. Biochem. 30*, 495−500.
4. Prince, R. C., Leigh, J. S., and Dutton, P. L. (1976) *Biochim. Biophys. Acta 440*, 622−636.
5. Lin, X., Murchison, H. A., Nagarajan, V., Parson, W. W., Allen, J. P., and Williams, J. C. (1994) *Proc. Natl. Acad. Sci. U.S.A. 91*, 10265−10269.
6. Tommos, C., and Babcock, G. T. (2000) *Biochim. Biophys. Acta 1458*, 199−219.
7. Kozlov, Y. N., Kazakova, A. A., and Klimov, V. V. (1997) *Membr. Cell Biol. 11*, 115−120.
8. Ananyev, G. M., Zaltsman, L., Vasko, C., and Dismukes, G. C. (2001) *Biochim. Biophys. Acta 1503*, 52−68.
9. Dismukes, G. C., Klimov, V. V., Baranov, S. V., Kozlov, Y. N., DasGupta, J., and Tyryshkin, A. (2001) *Proc. Natl. Acad. Sci. U.S.A. 98*, 2170−2175.
10. Klimov, V. V., Allakhverdiev, S. I., Feyziev, Y. M., and Baranov, S. V. (1995) *FEBS Lett. 363*, 251−255.
11. Klimov, V. V., Hulsebosch, R. J., Allakhverdiev, S. I., Wincencjusz, H., van Gorkom, H. J., and Hoff, A. J. (1997) *Biochemistry 36*, 16277−16281.
12. Williams, J. C., Alden, R. G., Murchison, H. A, Peloquin, J. M., Woodbury, N. W., and Allen, J. P. (1992) *Biochemistry 31*, 11029−11037.
13. Kleinherenbrink, F. A. M., Chiou, C. H., LoBrutto, R., and Blankenship, R. E. (1994) *Photosynth. Res. 41*, 115−123.
14. Allen, J. P., Williams, J. C., Graige, M. S., Paddock, M. L., Labahn, A., Feher, G., and Okamura, M. Y. (1998) *Photosynth. Res. 55*, 227−233.
15. Hoganson, C. W., Ghanotakis, D. F., Babcock, G. T., and Yocum, C. F. (1989) *Photosynth. Res. 22*, 285−293.
16. Maróti, P., and Wraight, C. A. (1988) *Biochim. Biophys. Acta 934*, 329−347.
17. Williams, J. C., Haffa, A. L. M., McCulley, J. L., Woodbury, N. W., and Allen, J. P. (2001) *Biochemistry 40*, 15403−15407.
18. Kálmán, L., LoBrutto, R., Allen, J. P., and Williams, J. C. (1999) *Nature 402*, 696−699.
19. Narváez, A. J., Kálmán, L., LoBrutto, R., Allen, J. P., and Williams, J. C. (2002) *Biochemistry 41*, 15253−15258.
20. Feher, G. (1971) *Photochem. Photobiol. 14*, 373−387.
21. Verméglio, A., and Clayton, R. K. (1977) *Biochim. Biophys. Acta 461*, 159−165.
22. Paddock, M. L., Graige, M. S., Feher, G., and Okamura, M. Y. (1999) *Proc. Natl. Acad. Sci. U.S.A. 96*, 6183−6188.
23. Haumann, M., Bögershausen, O., Cherepanov, D., Ahlbrink, R., and Junge, W. (1997) *Photosynth. Res. 51*, 193−208.
24. Velthuys, B. R. (1980) *Annu. Rev. Plant. Physiol. Plant. Mol. Biol. 31*, 545−567.
25. Hoganson, C. W., Casey, P. A., and Hansson, Ö. (1991) *Biochim. Biophys. Acta 1057*, 399−406.
26. Hammarström, L., Sun, L., Åkermark, B., and Styring, S. (2001) *Spectrochim. Acta A 57*, 2145−2160.
27. Baranov, S. V., Ananyev, G. M., Klimov, V. V., and Dismukes, G. C. (2000) *Biochemistry 39*, 6060−6065.
28. Kálmán, L., Gajda, T., Sebban, P., and Maróti, P. (1997) *Biochemistry 36*, 4489−4496.
29. Wydrzynski, T., and Govindjee (1975) *Biochim. Biophys. Acta 387*, 403−408.
30. Pierson, B. K. (1994) in *Early Life on Earth* (Bengston, S., Ed.) pp 161−180, Columbia University Press, NY.
31. Blankenship, R. B., and Hartman, H. (1998) *Trends Biol. Sci. 23*, 94−97.
32. Sauer, K., and Yachandra, V. K. (2002) *Proc. Natl. Acad. Sci. U.S.A. 99*, 8631−8636.
33. Gounot, A.-M. (1994) *FEMS Microbiol. Rev. 14*, 339−350.
34. Widdel, F., Schnell, S., Heising, S., Ehrenreich, A., Assmus, B., and Schink, B. (1993) *Nature 362*, 834−836.

BI034747O